

# Efficient semi-implicit schemes for stiff systems

Qing Nie <sup>\*</sup>, Yong-Tao Zhang, Rui Zhao

*Department of Mathematics, Center for Mathematical and Computational Biology, University of California, Irvine, 275  
MSTB, Irvine, CA 92697-3875, United States*

Received 15 April 2005; received in revised form 15 September 2005; accepted 29 September 2005  
Available online 15 November 2005

---

## Abstract

When explicit time discretization schemes are applied to stiff reaction–diffusion equations, the stability constraint on the time step depends on two terms: the diffusion and the reaction. The part of the stability constraint due to diffusion can be totally removed if the linear diffusions are treated exactly using integration factor (IF) or exponential time differencing (ETD) methods. For systems with severely stiff reactions, those methods are not efficient because the reaction terms in IF or ETD are still approximated with explicit schemes. In this paper, we introduce a new class of semi-implicit schemes, which treats the linear diffusions exactly and explicitly, and the nonlinear reactions implicitly. A distinctive feature of the scheme is the decoupling between the exact evaluation of the diffusion terms and implicit treatment of the nonlinear reaction terms. As a result, the size of the nonlinear system arising from the implicit treatment of the reactions is independent of the number of spatial grid points; it only depends on the number of original equations, unlike the case in which standard implicit temporal schemes are directly applied to the reaction–diffusion system. The stability region for this class of methods is much larger than existing methods using an explicit treatment of reaction terms. In particular, the one with second order accuracy is unconditionally linearly stable with respect to both diffusion and reaction. Direct numerical simulations on test equations, as well as morphogen systems from developmental biology, show the new semi-implicit schemes are efficient, robust and accurate.

© 2005 Elsevier Inc. All rights reserved.

*Keywords:* Implicit schemes; Reaction–diffusion equations; Morphogen gradients

---

## 1. Introduction

Mathematical equations for many physical and biological applications are of the form:

$$\frac{\partial \mathbf{u}}{\partial t} = D\Delta \mathbf{u} + \mathbf{F}(\mathbf{u}), \quad (1)$$

---

<sup>\*</sup> Corresponding author. Tel.: +1 949 824 5530; fax: +1 949 824 7993.  
E-mail address: [qnie@math.uci.edu](mailto:qnie@math.uci.edu) (Q. Nie).

where  $\mathbf{u} \in \mathbf{R}^m$  represents a group of physical or biological species,  $D \in \mathbf{R}^{m \times m}$  is the diffusion constant matrix,  $\Delta \mathbf{u}$  is the Laplacian associated with the diffusion of the species  $\mathbf{u}$ , and  $\mathbf{F}(\mathbf{u})$  describes the chemical or biological reactions.

If the method of lines is used to solve the equation numerically, the reaction–diffusion system (1) can be reduced to a system of ODEs:

$$u_t = \mathcal{C}u + \mathcal{F}(u), \quad (2)$$

where  $\mathcal{C}u$  is a finite difference approximation of  $D\Delta \mathbf{u}$ . Let  $N$  denote the number of spatial grid points (independent of number of spatial dimensions) for the approximation of the Laplacian  $\Delta \mathbf{u}$ . Then  $u(t) \in \mathbf{R}^{N \cdot m}$  and  $\mathcal{C}$  is a  $(N \cdot m) \times (N \cdot m)$  matrix representing a spatial discretization of the diffusion. For instance, in a one-dimensional system with one diffusion term,  $\mathcal{C}$  is a tri-diagonal matrix when a second order central difference is used. The eigenvalues of  $\mathcal{C}$  are proportional to  $DN^2$  in this case.

The size of time-step for a time integrator solving, Eq. (2), is constrained by the inverse of the eigenvalues of the diffusion matrix  $\mathcal{C}$  in addition to the stiffness of the nonlinear reaction term  $\mathcal{F}(u)$ . When diffusion constants in system (1) become large or the spatial resolution is very fine as  $N$  increases, the stability constraint due to diffusion becomes very severe. However, this constraint due to diffusion can be totally removed by treating the term  $\mathcal{C}u$  exactly [1–3]. In this approach, the contribution of the linear diffusion is reduced to evaluation of an exponential function of the matrix  $\mathcal{C}$ , followed by an approximation of an integral involving the nonlinear term  $\mathcal{F}(u)$ . Different approximations of the integral involving nonlinear term  $\mathcal{F}(u)$  result in either the integration factor (IF) method or the exponential time differencing (ETD) method. For ETD methods, special treatments for various operations on  $\mathcal{C}$  (e.g., its inverse) are needed in order to maintain a consistent order of accuracy [4–7]. For standard IF methods, the fixed points for the original systems are not *exactly* conserved in the numerical scheme, and as a result, extra terms have to be incorporated in the standard IF methods in order to preserve such conservation [8].

Although the stability constraint due to diffusion is totally removed for IF and ETD methods, the time step is still constrained by the stiffness of the reaction term  $\mathcal{F}(u)$ . This is because in classical IF and ETD methods, the term  $\mathcal{F}(u)$  is usually treated explicitly through linear multi-step methods, such as Adams–Bashforth methods [1,3]. One way of improving the stability region for a stiff reaction is to incorporate a Runge–Kutta type approximation for the term involving  $\mathcal{F}(u)$  in the ETD scheme [9]. Although the multi-stage nature of Runge–Kutta methods requires more function evaluations, the ETD–Runge–Kutta method [9] in general has a larger stability region than the standard ETD [3]. However, it is still not efficient enough for systems with highly stiff reactions, as often is the case for many biological applications, such as the morphogen gradient system in which the reaction rate constants in  $\mathbf{F}(u)$  can differ by four to five order of magnitude [10–13].

On the other hand, direct application of classical implicit temporal schemes on (2) leads to a large system of  $N \cdot m$  equations and  $N \cdot m$  unknowns. The size of the system depends on the spatial resolution  $N$ , which represents the total number of spatial grid points independent of the number of spatial dimensions. The computational cost for solving such system is of order of  $N^2 \cdot m^2$  if Newton's methods is used. (Of course, fast methods, such as the multigrid methods, can significantly speed up these calculations.) In this paper, we introduce a new class of methods, which treats the diffusion term exactly and the nonlinear reaction term  $\mathcal{F}(u)$  implicitly, *but* with the two approximations decoupled. By doing so, we only need to solve a system of  $m$  equations and  $m$  unknowns at every spatial grid point. The computational cost for solving the system at one spatial point is of order of  $m^2$  using iterative methods such as Newton's methods. Summing up this computational cost at all spatial points, the total cost for solving all  $N$  systems becomes order of  $N \cdot m^2$ . In addition, the small system of  $m$  equations and  $m$  unknowns is convenient for the implementation of various nonlinear solvers, and it is in a form particularly suitable for a simple fixed point iterative procedure.

With the implicit treatment of the nonlinear reactions, the new methods have a much larger stability region than the ETD–Runge–Kutta method [9]; in particular, its second order version is unconditionally linearly stable with respect to both diffusion and reactions. In this paper, we present two types of methods: the basic type, which can be regarded as an implicit integration factor (IIF) method, and an advanced type, which combines the IIF method and standard explicit ETD methods through appropriate weights to ensure the conservation of fixed points of the numerical schemes. It will be demonstrated that the IIF method is more efficient and robust

than the weighted scheme, and IIF method performs well for a system of PDEs arising from a biological application.

The rest of the paper is organized as following. In Section 2, we derive the IIF method. In Section 3, we analyze the linear stability for IIF. In Section 4, we present the weighted IIF-ETD methods, and discuss their stability properties. In Section 5, we test and compare the new methods with some existing methods for a system of PDEs with an exact solution. In Section 6, we apply IIF to a morphogen system in developmental biology. In Section 7, we conclude.

## 2. Implicit integrating factor methods

In this section, we illustrate the derivation of the new temporal schemes for the scalar case of the semi-discrete system (2) of the form

$$u_t = cu + f(u), \quad t > 0, \quad u(0) = u_0, \tag{3}$$

where  $c$  is a constant representing the diffusion, and  $f$  is a nonlinear function representing the reaction.

After multiplying (3) by the integrating factor  $e^{-ct}$ , we integrate the equation over one time step from  $t_n$  to  $t_{n+1} \equiv t_n + \Delta t$  to obtain

$$u(t_{n+1}) = u(t_n)e^{c\Delta t} + e^{c\Delta t} \int_0^{\Delta t} e^{-c\tau} f(u(t_n + \tau)) \, d\tau. \tag{4}$$

One critical step in constructing ETD schemes [2,3,9] is the choice of approximation method for the integral in (4). In the derivation of ETD schemes, the integrand is approximated first through interpolation polynomials of the function  $f(u(t_n + \tau))$  with  $e^{-c\tau}$  unchanged. Then a direct integration of the interpolation polynomial with a coefficient  $e^{-c\tau}$  yields the ETD method. If the interpolation points used for the integrand are at  $\tau \leq 0$ , the temporal scheme is explicit. Otherwise, the scheme becomes implicit when the interpolation points contain  $t_{n+1}$ . The implicit treatment of the reaction term  $f$  gives a much larger stability region for stiff reactions compared to the explicit ETD schemes.

However, the nonlinear equation arising from those implicit ETD methods [3] involves a term  $e^{c\Delta t}f(u_{n+1})$ . For example, the second order implicit ETD scheme is of the form:

$$u_{n+1} = e^{c\Delta t}u_n + \frac{e^{c\Delta t} - 1}{2c} (f(u_{n+1}) + f(u_n)). \tag{5}$$

When the implicit ETD scheme (5) applied to an ODE system (2), it leads to a nonlinear system with  $N \cdot m$  equations and  $N \cdot m$  unknowns, where  $N$  represents the number of spatial discretization points for diffusion, and  $m$  represents the number of original differential equations. This system, which couples the linear diffusion and the nonlinear reaction through exponentials of matrix  $\mathcal{C}$ , is generally expensive to solve. The computational complexity for solving the system is of order at least  $O(N^2 \cdot m^2)$  using a standard iterative method (e.g., Newton’s method).

Our goal is to design a class of temporal schemes which treats the stiff reaction implicitly and integrates the diffusion exactly, but with a much reduced computational cost. In particular, it would be desirable to decouple the treatment of stiff reactions and the exact integration of diffusion so that a nonlinear system of only  $m$  equations with  $m$  unknowns needs to be solved at every spatial grid point, with the size of the nonlinear system independent of the total number of the grid points  $N$ . It turns out we can construct such a scheme by simply approximating  $e^{-c\tau}f(u(t_n + \tau))$  in (4) using an interpolation polynomial involving  $t_{n+1}$ . Here is a brief description of the derivation.

Define  $u_n$  as the numerical solution for  $u(t_n)$  and

$$g(\tau) = e^{-c\tau}f(u(t_n + \tau)). \tag{6}$$

To construct a scheme of  $r$ th order truncation error, we approximate  $g(\tau)$  with an  $r - 1$ th order Lagrange polynomial,  $p(\tau)$ , with interpolation points at  $t_{n+1}, t_n, \dots, t_{n+2-r}$ :

$$p(\tau) = \sum_{i=-1}^{r-2} e^{ic\Delta t} f(u_{n-i}) \prod_{\substack{j=-1 \\ j \neq i}}^{r-2} \frac{\tau + j\Delta t}{(j-i)\Delta t}, \quad 0 \leq \tau \leq \Delta t. \tag{7}$$

Then the second, third, and fourth order approximations to  $g(\tau)$  are of the following form:

1. Given  $g(0) = f(u_n)$ ,  $g(\Delta t) = e^{-c\Delta t} f(u_{n+1})$ , the second order approximation to  $g(\tau)$  is

$$p(\tau) = \frac{1}{\Delta t} [f(u_n)(\Delta t - \tau) + e^{-c\Delta t} f(u_{n+1})\tau], \quad 0 \leq \tau \leq \Delta t. \tag{8}$$

2. Given  $g(-\Delta t) = e^{c\Delta t} f(u_{n-1})$ ,  $g(0) = f(u_n)$ ,  $g(\Delta t) = e^{-c\Delta t} f(u_{n+1})$ , the third order approximation to  $g(\tau)$  is

$$p(\tau) = \frac{1}{2\Delta t^2} [e^{c\Delta t} f(u_{n-1})\tau(\tau - \Delta t) - 2f(u_n)(\tau + \Delta t)(\tau - \Delta t) + e^{-c\Delta t} f(u_{n+1})\tau(\tau + \Delta t)], \quad 0 \leq \tau \leq \Delta t. \tag{9}$$

3. Given  $g(-2\Delta t) = e^{2c\Delta t} f(u_{n-2})$ ,  $g(-\Delta t) = e^{c\Delta t} f(u_{n-1})$ ,  $g(0) = f(u_n)$ ,  $g(\Delta t) = e^{-c\Delta t} f(u_{n+1})$ , the fourth order approximation to  $g(\tau)$  is

$$p(\tau) = \frac{1}{6\Delta t^3} [-e^{2c\Delta t} f(u_{n-2})(\tau - \Delta t)\tau(\tau + \Delta t) + 3e^{c\Delta t} f(u_{n-1})(\tau - \Delta t)\tau(\tau + 2\Delta t) - 3f(u_n)(\tau - \Delta t)(\tau + \Delta t)(\tau + 2\Delta t) + e^{-c\Delta t} f(u_{n+1})\tau(\tau + \Delta t)(\tau + 2\Delta t)], \quad 0 \leq \tau \leq \Delta t. \tag{10}$$

With this approximation to  $g(\tau)$ , (4) can be discretized as

$$u_{n+1} = e^{c\Delta t} u_n + e^{c\Delta t} \int_0^{\Delta t} p(\tau) d\tau. \tag{11}$$

Hence, a direct evaluation of the integral in (11) leads to the new  $r$ th order implicit scheme

$$u_{n+1} = e^{c\Delta t} u_n + \Delta t \left( \alpha_{n+1} f(u_{n+1}) + \sum_{i=0}^{r-2} \alpha_{n-i} f(u_{n-i}) \right), \tag{12}$$

with  $\alpha_{n+1}, \alpha_n, \alpha_{n-1}, \dots, \alpha_{n-r+2}$  defined as

$$\alpha_{n-i} = \frac{e^{(i+1)c\Delta t}}{\Delta t} \int_0^{\Delta t} \prod_{\substack{j=-1 \\ j \neq i}}^{r-2} \frac{\tau + j\Delta t}{(j-i)\Delta t} d\tau, \quad -1 \leq i \leq r-2. \tag{13}$$

In Table 1, we list the value of coefficients,  $\alpha_j$ , for the schemes with order up to four. For example, the second order scheme is of the following form:

$$u_{n+1} = e^{c\Delta t} \left( u_n + \frac{\Delta t}{2} f(u_n) \right) + \frac{\Delta t}{2} f(u_{n+1}), \tag{14}$$

with a local truncation error

$$-\frac{1}{12} (c^2 f_n - 2c \dot{f}_n + \ddot{f}_n) \Delta t^3. \tag{15}$$

Table 1  
Coefficients for implicit IF schemes with localized nonlinear systems

Order	$\alpha_{n+1}$	$\alpha_n$	$\alpha_{n-1}$	$\alpha_{n-2}$
1	1	0	0	0
2	$\frac{1}{2}$	$\frac{1}{2}e^{c\Delta t}$	0	0
3	$\frac{5}{12}$	$\frac{7}{6}e^{c\Delta t}$	$-\frac{1}{12}e^{2c\Delta t}$	0
4	$\frac{9}{24}$	$\frac{19}{24}e^{c\Delta t}$	$-\frac{5}{24}e^{2c\Delta t}$	$\frac{1}{24}e^{3c\Delta t}$

The distinctive feature of the scheme (12) and (13) is that  $\alpha_{n+1}$  is independent of  $e^{c\Delta t}$  unlike the implicit ETD (5). As a result, when the scheme is applied to the ODE system of the form (2), the exponential matrix  $e^{c\Delta t}$  is only multiplied by terms involving known quantities at the earlier time levels. The nonlinear system at  $t_{n+1}$  is decoupled from the diffusion with a simple form

$$\mathbf{u}_{n+1} = \Delta t \alpha_{n+1} \mathcal{F}(\mathbf{u}_{n+1}) + \text{known quantities} \tag{16}$$

with  $\mathbf{u}_{n+1} \in \mathbf{R}^m$ . At each time step for the IIF (14), a system with  $m$  unknowns (16) needs to be solved at each spatial grid point. The  $Nm \times m$  systems are independent of each other with every system of the same structure. Because  $\Delta t \alpha_{n+1} \ll 1$ ,  $\Delta t \alpha_{n+1} \mathcal{F}$  in (16) is likely to be a contractive mapping [14], and an iterative method such as the fixed point method is particularly suitable and convenient to implement for the corresponding nonlinear system.

Unlike ETD schemes [2,3,9], the new schemes do *not* involve any calculation of  $\mathcal{C}^{-1}$ . Direct implementation of ETD schemes [2,3,9] usually suffers from numerical instability due to large cancellation errors. Special care must be taken for the calculation of  $\mathcal{C}^{-1}$ , especially when  $\mathcal{C}$  has zero or close to zero eigenvalues [4]. The new IIF scheme only involves calculation of  $e^{c\Delta t}$ , a term independent of  $\mathbf{u}$  or  $\mathcal{F}$ . This term can be pre-calculated for a given numerical resolution (fixed  $N$  and  $\Delta t$ ), and stored for later use at every time step. A comprehensive discussion on evaluation of the exponential of a matrix can be found in [15]. In this paper, we use a scaling and squaring algorithm with a Padé approximation [15] implemented in Matlab with the function name “expm”.

**Remark.** The procedure of using (4) to obtain the IIF methods can also be applied for construction of explicit integration factor (EIF) methods. With interpolation points involving points with  $\tau \leq 0$ , we can obtain the  $r$ th order EIF as the following:

$$u_{n+1} = e^{c\Delta t} u_n + \Delta t \left( \sum_{i=0}^{r-1} \beta_{n-i} f(u_{n-i}) \right), \tag{17}$$

where

$$\beta_{n-i} = \frac{e^{(i+1)c\Delta t}}{\Delta t} \int_0^{\Delta t} \prod_{\substack{j=0 \\ j \neq i}}^{r-1} \frac{\tau + j\Delta t}{(j-i)\Delta t} d\tau, \quad 0 \leq i \leq r-1. \tag{18}$$

For the case  $r = 2$ , it is reduced to the standard second order integration factor Adams–Bashforth method (IFAB2 [9]):

$$u_{n+1} = e^{c\Delta t} u_n + \Delta t \left( \frac{3}{2} e^{c\Delta t} f(u_n) - \frac{1}{2} e^{2c\Delta t} f(u_{n-1}) \right). \tag{19}$$

So Eq. (4) is a general framework for both explicit and implicit ETD schemes and IF methods. The choice of approximation procedure for the integrand in (4) dictates the type of temporal schemes derived. The ETD schemes are obtained when  $f(u(t_n + \tau))$  is approximated through interpolation polynomials, whereas the IF method is obtained when the whole integrand  $e^{-c\tau} f(u(t_n + \tau))$  is approximated.

### 3. Stability analysis of IIF

One of the drawbacks for standard integrating factor methods is that the fixed points of the numerical schemes are not the same as the fixed points of the original ODEs; and they differ by a term of order  $(\Delta t^p)$  where  $p$  is the order of accuracy of the numerical scheme. In other words, the steady state obtained from a dynamic evolution using standard integration factor methods has an error of order  $(\Delta t^p)$  in addition to discretization errors associated with space. This error is more pronounced for PDEs involving higher-order spatial derivatives, such as applications in microstructure evolution [8,16].

Because the fixed points of the numerical scheme are not conserved, one cannot directly use the following decoupled linear system:

$$u_t = -qu + du \quad \text{with } q > 0 \tag{20}$$

to examine the stability region with respect to the diffusion and the reaction for the implicit integration factor method around the steady state of the ODE system (2) as shown in [3,17]. Instead, one may analyze the linear stability of integration factor methods around the steady state of the numerical schemes. Interestingly this approach happens to be equivalent to testing the stability of the numerical methods using such a linear system as (20). Similar to the stability analysis for ETD methods in [3,17], we will show boundaries of the stability region, a family of curves for different values of  $q\Delta t$ , based on the test problem (20) for the second and third order implicit integration factor methods. In the context of solving reaction–diffusion equation (1) using a finite difference scheme for the spatial discretization,  $q\Delta t$  actually represents the CFL number involving the ratio of the temporal and spatial grid size.

Applying the second order IIF (14) to Eq. (20), then substituting  $u_n = e^{in\theta}$  into the resulting equation, we obtain

$$e^{i\theta} = e^{-q\Delta t} \left( 1 + \frac{1}{2}\lambda \right) + \frac{1}{2}\lambda e^{i\theta}, \tag{21}$$

where  $\lambda = d\Delta t$  has a real part  $\lambda_r$  and imaginary part  $\lambda_i$ . Therefore, the equations for  $\lambda_r$  and  $\lambda_i$  are

$$\begin{aligned} \lambda_r &= \frac{2(1 - e^{-2q\Delta t})}{(1 - e^{-q\Delta t})^2 + 2(1 + \cos \theta)e^{-q\Delta t}}, \\ \lambda_i &= \frac{4(\sin \theta)e^{-q\Delta t}}{(1 - e^{-q\Delta t})^2 + 2(1 + \cos \theta)e^{-q\Delta t}}. \end{aligned} \tag{22}$$

Because  $q > 0$ , we have  $\lambda_r > 0$  for  $0 \leq \theta \leq 2\pi$ . Then, the second order IIF is  $A$ -stable since the stability region includes the complex plane for all  $\lambda$  with  $\lambda_r < 0$ . In Fig. 1, we plot the stability regions: the exterior of the closed curves located on the complex plane with  $\lambda_r > 0$ , for  $q\Delta t = 0.5, 1, 2$ . In the limit  $q \rightarrow 0$ , the stability region coincides with the domain  $\lambda_r < 0$ , whereas in the limit  $q \rightarrow \infty$ , the stability region approaches the whole complex plane excluding the point  $(2, 0)$ .

Next, we examine the third order IIF scheme:

$$u_{n+1} = e^{c\Delta t}u_n + \Delta t \left( \frac{5}{12}f(u_{n+1}) + \frac{2}{3}e^{c\Delta t}f(u_n) - \frac{1}{12}e^{2c\Delta t}f(u_{n-1}) \right). \tag{23}$$

Using the same approach, we obtain the equation for  $\lambda$

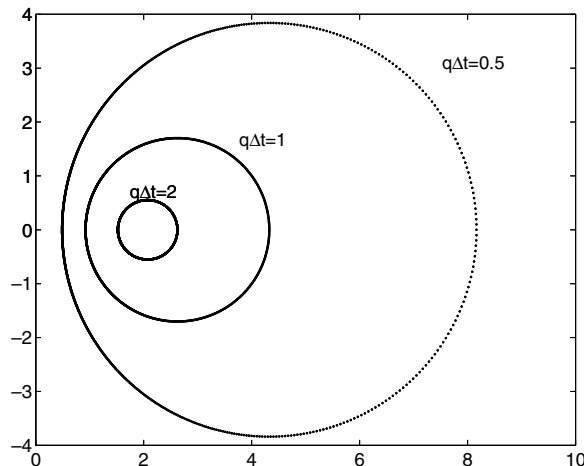


Fig. 1. Stability regions (exterior of the closed curves) for the second order IIF with  $q\Delta t = 0.5, 1, 2$ .

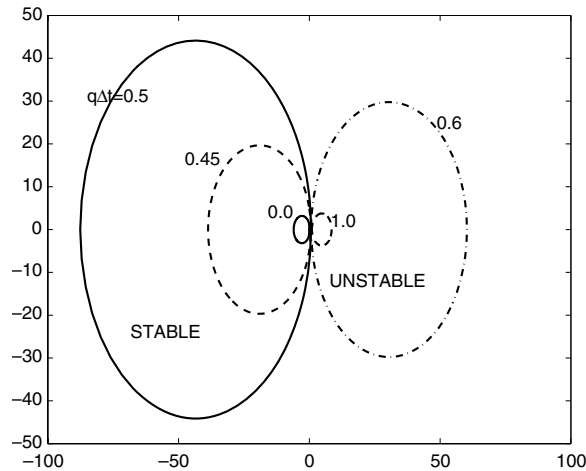


Fig. 2. Stability regions for the third order IIF scheme with  $q\Delta t = 0, 0.45, 0.5, 0.6, 1.0$ .

$$\lambda = \frac{e^{i\theta} - e^{-q\Delta t}}{\frac{5}{12}e^{i\theta} + \frac{2}{3}e^{-q\Delta t} - \frac{1}{12}e^{-2q\Delta t - i\theta}} \tag{24}$$

The third order scheme is no longer A-stable, as shown in Fig. 2 for  $q\Delta t = 0, 0.45, 0.5, 0.6, 1.0$ . The stability region of IIF is larger than the corresponding implicit ETD scheme [3] for every fixed  $q\Delta t$ . However, the size of the stability region is very sensitive to the value of  $q\Delta t$ , and it is an increasing function of  $q\Delta t$ .

When  $q\Delta t < 0.54$ , the stability region is within the left of the complex plane  $\lambda$  bounded by a closed curve. When  $q\Delta t > 0.55$ , the stability region contains the whole left of the plane and most of the right part of the plane. As  $q \rightarrow \infty$ , the stability region approaches the whole complex plane excluding one point at the real axis.

#### 4. Weighted implicit integration factor and exponential time differencing methods (wIIF-ETD)

As discussed in the previous section, one of the main drawbacks for the standard integration factor methods is that the fixed points of the discrete equations from the numerical methods has an error of  $O(\Delta t^p)$  where  $p$  is the order of accuracy of the numerical scheme. This problem can be eliminated through addition of appropriate terms in the original scheme for the second order explicit integration factor method when applied to a boundary integral technique [16]. In this section, we will introduce a new class of schemes combining IIF and ETD such that the fixed points of the new schemes are conserved with a stability region comparable to the new IIF.

We illustrate the construction of the new scheme by deriving a weighted formula from the second order IIF and the second order ETD. Define two weights  $w_1$  and  $w_2$  for IIF and ETD, respectively. Then, Eq. (4) becomes

$$u(t_{n+1}) = u(t_n)e^{c\Delta t} + w_1 \left( e^{c\Delta t} \int_0^{\Delta t} e^{-c\tau} f(u(t_n + \tau)) d\tau \right) + w_2 \left( e^{c\Delta t} \int_0^{\Delta t} e^{-c\tau} f(u(t_n + \tau)) d\tau \right). \tag{25}$$

Approximating the integral in the  $w_1$  term using the second order IIF approach and the integral in the  $w_2$  term using the second order ETD approach, we obtain

$$u_{n+1} = e^{c\Delta t}u_n + w_1 \left[ \frac{\Delta t}{2}f(u_{n+1}) + \frac{\Delta te^{c\Delta t}}{2}f(u_n) \right] + w_2 \left[ \frac{(1 + c\Delta t)e^{c\Delta t} - 1 - 2c\Delta t}{c^2\Delta t}f(u_n) + \frac{-e^{c\Delta t} + 1 + c\Delta t}{c^2\Delta t}f(u_{n-1}) \right]. \tag{26}$$

Denote  $u^*$  as the fixed point of Eq. (26) (setting  $u_{n+1} = u_n = u_{n-1} = u^*$ ), and  $\bar{u}$  as the fixed point of the original PDEs (3) (setting  $c\bar{u} = -f(\bar{u})$ ). Then  $u^* = \bar{u}$  yields

$$w_2 = 1 - \frac{c\Delta t}{2} \cdot \frac{e^{c\Delta t} + 1}{e^{c\Delta t} - 1} w_1. \tag{27}$$

Because  $w_1 + w_2 = 1 + O(\Delta t^2)$ , the scheme (26) clearly has second order accuracy. If the weight  $w_1$  is chosen as a free parameter, we have a class of new schemes based on the choice of  $w_1$ . When  $w_1 = 0$ , the scheme becomes the ETD. No  $w_1$  can be chosen to reproduce IIF since the fixed points of IIF are not conserved, but the fixed points of the new scheme (26) are. Most importantly, in the new scheme there are no terms involving  $c$  or exponentials of  $c$  in front of  $f(u_{n+1})$  as is the case with the IIF scheme. To examine the stability of the scheme (26), we now perform the standard approach using (20) [3,17] because the fixed points of the discrete equation are the same as the original PDEs. In the stability analysis,  $c = -q$  and  $q > 0$  in the definition of  $w_2$ , and  $w_1$  must satisfy

$$0 \leq w_1 \leq \frac{2(1 - e^{-q\Delta t})}{q\Delta t(1 + e^{-q\Delta t})} \equiv W(q\Delta t) \tag{28}$$

for any fixed  $q\Delta t$  in order to make  $w_1$  and  $w_2$  both positive. Consequently, we also have  $0 \leq w_2 \leq 1$ .

One of the important properties for the function  $W$  is that  $W(\alpha) < 1$  for  $\alpha > 0$ . This can be proved by showing  $f(\alpha) \equiv 2(1 - e^{-\alpha}) - \alpha(1 + e^{-\alpha})$  is a decreasing function for  $\alpha \geq 0$ .  $W(\alpha) < 1$  then follows from  $f(\alpha) < f(0) = 0$  for  $\alpha > 0$ . In addition, we have  $W(\alpha) \rightarrow 1$  as  $\alpha \rightarrow 0$  and  $W(\alpha) \rightarrow 0$  as  $\alpha \rightarrow \infty$ . Using those properties, we can easily show

$$0 \leq w_1 + w_2 \leq 1 \tag{29}$$

for any  $q\Delta t > 0$  as long as  $0 \leq w_1 \leq W(q\Delta t)$ .

Now using (20) with  $u_n = e^{i\theta}$  and  $\lambda = d\Delta t$ , we obtain

$$\lambda = \frac{e^{i\theta} - e^{-\alpha}}{\frac{w_1}{2} [e^{i\theta} + e^{-\alpha}] + \left(1 + \frac{\alpha(e^{-\alpha} + 1)}{2(e^{-\alpha} - 1)} w_1\right) \left[\frac{(1-\alpha)e^{-\alpha} - 1 + 2\alpha}{\alpha^2} + \frac{1-\alpha-e^{-\alpha}}{\alpha^2} e^{-i\theta}\right]}, \tag{30}$$

where  $\alpha = q\Delta t$ .

In Fig. 3, we plot the stability region for various  $w_1$ , the weight for the IIF scheme. When  $w_1 = 0$ , the stability region is reduced to that of the ETD scheme. As  $w_1$  increases, corresponding to a larger weight on IIF, the stability region becomes larger until it reaches the required upper limit  $W(q\Delta t)$ , at which the stability region is the largest among all  $w_1$ . In fact, it can be shown easily that the stability region for  $w_1 = W(q\Delta t)$

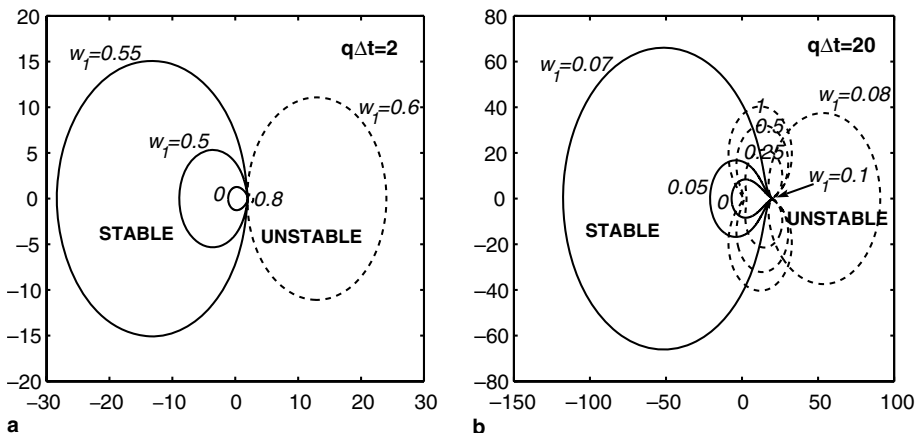


Fig. 3. Stability regions for the second order weighted IIF-ETD scheme. Different curves correspond to different implicit parameter  $w_1$ . The interior of the solid curve is the region of stability and the exterior of the dashed curve is the region of stability. (a)  $q\Delta t = 2$ , solid curves:  $w_1 = 0, 0.5, 0.55$  and the dashed curves:  $w_1 = 0.6, 0.8$ . (b)  $q\Delta t = 20$ , solid curves:  $w_1 = 0, 0.05, 0.07$  and the dashed curves:  $w_1 = 0.08, 0.1, 0.25, 0.5, 1$ .

includes the whole left part of the  $\lambda$  complex plane similar to the IIF. In Fig. 3,  $W(2) \approx 0.8$  and  $W(20) \approx 0.1$ . Similar to IIF and ETD, the size of the stability region is an increasing function of  $q\Delta t$ .

**Remark.** One alternative to designing a numerical scheme with conserved fixed points is to combine the implicit IF method with the explicit IF method, instead of explicit ETD method as discussed above. Although the fixed points for either scheme are not conserved, their combination can be. We illustrate this idea by analyzing a second order version of this weighted IIF and explicit IF scheme.

Introducing two weights,  $w_1$  for the IIF and  $w_2$  for the explicit IF, we obtain the weighted scheme of the form:

$$u_{n+1} = e^{c\Delta t}u_n + w_1 \left[ \frac{\Delta t}{2}f(u_{n+1}) + \frac{\Delta te^{c\Delta t}}{2}f(u_n) \right] + w_2 \left[ \frac{3\Delta t}{2}e^{c\Delta t}f(u_n) - \frac{\Delta t}{2}e^{2c\Delta t}f(u_{n-1}) \right]. \tag{31}$$

In order for  $u_{n+1} = u_n = u_{n-1} = u^*$  in (31) at its steady state equal to the steady state of the original ODEs (3), one has to require

$$w_2 = \frac{1}{3 - e^{c\Delta t}} \left[ \frac{2(1 - e^{-c\Delta t})}{c\Delta t} - (1 + e^{-c\Delta t})w_1 \right]. \tag{32}$$

The scheme (31) has second order accuracy and its weights satisfy the following relationship:

$$w_1 + w_2 = 1 + \frac{5c^2\Delta t^2}{12 - 6c\Delta t} - \frac{c^2\Delta t^2}{2 - c\Delta t}w_1 + O(\Delta t^3). \tag{33}$$

Because the term  $e^{-c\Delta t}$  in  $w_2$  grows exponentially as a function of  $\Delta t$  for  $c < 0$ , which is the case for a reaction–diffusion system,  $w_2$  will be extremely sensitive to the choice of  $\Delta t$ . In addition,  $w_1 + w_2$  grows linearly as the speed of diffusion,  $|c|$ , unlike the weighted IIF-ETD scheme, which has a uniform upper bound. These drawbacks together make the weighted IIF-IF scheme numerically unstable and impractical to use.

### 5. Tests on a reaction–diffusion system

In this section, we test the new schemes derived in Sections 2 and 4, and compare them to existing schemes for a reaction–diffusion system with an exact solution. The one-dimensional reaction–diffusion system of two unknowns has absorbing boundary conditions at one end and no-flux boundary conditions at the other end:

$$\begin{aligned} u_t &= du_{xx} - au + v, & 0 < x < \frac{\pi}{2}, \\ v_t &= dv_{xx} - bv, & 0 < x < \frac{\pi}{2}, \\ u_x|_{x=0} &= 0, & v_x|_{x=0} &= 0, \\ u|_{x=\frac{\pi}{2}} &= 0, & v|_{x=\frac{\pi}{2}} &= 0. \end{aligned} \tag{34}$$

The linearity of the reactions in (34) allows one to construct an exact solution:

$$\begin{aligned} u(x, t) &= (e^{-(a+d)t} + e^{-(b+d)t}) \cos(x), \\ v(x, t) &= (a - b) e^{-(b+d)t} \cos(x). \end{aligned} \tag{35}$$

A second order central difference is used for approximation of  $u_{xx}$  with a consistent approximation on the no-flux boundary condition. Let  $\Delta x = 0.5\pi/(N + 1)$  where  $N + 2$  is the total number of mesh points in  $[0, \pi/2]$ , so the semi-discretization of (34) is in the form of (2) with  $m = 2$ . The matrix  $\mathcal{C}$  is a diagonal matrix in a block structure with the same diagonal element,  $(d/\Delta x^2)\mathcal{A}_{N \times N}$ , where  $\mathcal{A}$  is a tri-diagonal matrix with  $-2$  at the diagonal entry and 1 at the off-diagonal entry, except for the two-non-zero entries in the first row due to the no-flux boundary condition.

As a result, the exponential of  $\mathcal{C}$  in (14) is reduced to the exponential of  $(d/\Delta x^2)\mathcal{A}$ , which can be computed using the scaling and squaring algorithm with a Padé approximation [15] as implemented in “expm” of

Matlab. Since  $\mathcal{C}$  only depends on  $\Delta x$  and  $d$ , this calculation needs to be done once initially at  $t = 0$  for the entire temporal updating.

First, we test the order of accuracy for the second order IIF (14) for two sets of reaction rates and diffusion coefficients. For both cases,  $a = 100$  is fixed so the smallest eigenvalue associated with the reaction is  $-100$ . In Table 2, we list the maximum error between the numerical solution and the exact solution, and the order of accuracy. The spatial resolution,  $N = 575$ , is chosen fine enough such that the error is dominated by the time step. Clearly, the order of accuracy in time for the IIF is two as demonstrated in Table 2. Notice that the largest eigenvalue for the reaction terms is  $-1$  for the first case and  $-0.01$  for the second case. The discretized diffusion matrix  $\mathcal{C}$  is the same for both cases with the largest eigenvalue  $-10^{-3}$  and the smallest eigenvalue  $-538$ . Therefore, the semi-discretized system is stiff in both diffusion and reaction, with the stiffness in diffusion slightly stronger than the reaction term.

For comparison, we next implement the second order Runge–Kutta, ETD [9], ETD–Runge–Kutta [9], the second order additive implicit–explicit Runge–Kutta method (ASIRK-2A) [18,19], the new IIF, the new weighted IIF-ETD for the system (34). For the ASIRK-2A method, we implement two versions: one with an implicit treatment on the reaction and an explicit treatment on the diffusion (ASIRK-2A-R), and the other with an implicit treatment on the diffusion and an explicit treatment on the reaction (ASIRK-2A-D). In Fig. 4, the maximum error between the exact solution and the numerical solution is plotted as a function of time step in a log–log scale for those schemes.

As expected, the standard Runge–Kutta method quickly blows up as  $\Delta t$  increases. The size of  $\Delta t$  for this method is controlled by the stiffness of the diffusion since the diffusion matrix is slightly more stiff than the reaction in the test problem. Similarly, the ASIRK-2A-R blows up around the same  $\Delta t$  as in this method the diffusion is still treated using explicit Runge–Kutta although the reaction is treated implicitly.

On the other hand, the ETD scheme is unconditionally stable with respect to the diffusion, but it still blows up at a slightly larger  $\Delta t$  due to the stiffness of the reaction since the scheme uses the explicit Adams–Bashforth method for the reaction. Because the Runge–Kutta method has a larger stability region than the Adams–Bash-

Table 2  
Errors and order of accuracy for the second order IIF

$\Delta t$	$b = 1, d = 10^{-3}$		$b = 10^{-2}, d = 1$	
	$L^\infty$ error	Order	$L^\infty$ error	Order
$4.0 \times 10^{-2}$	$4.85 \times 10^{-3}$	2.00	$3.42 \times 10^{-4}$	1.96
$2.0 \times 10^{-2}$	$1.21 \times 10^{-3}$	1.99	$8.79 \times 10^{-5}$	1.98
$1.0 \times 10^{-2}$	$3.03 \times 10^{-4}$	2.00	$2.23 \times 10^{-5}$	1.97
$5.0 \times 10^{-3}$	$7.58 \times 10^{-5}$	2.00	$5.67 \times 10^{-6}$	1.98

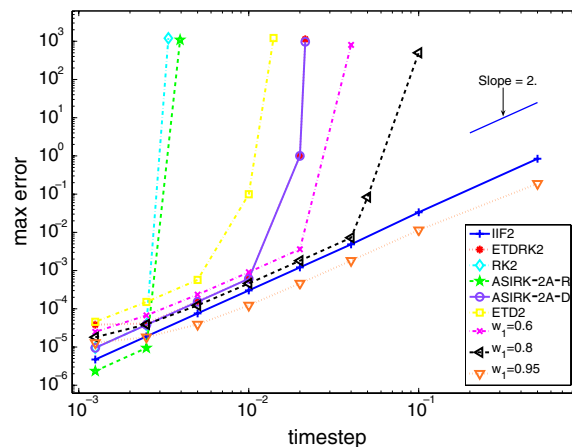


Fig. 4. Error as a function of time step for various schemes with a second order of accuracy.

forth method, the ETD-Runge–Kutta method [9], in which the reaction is treated using the explicit Runge–Kutta, converges for an even larger range of  $\Delta t$ . Similar to the ETD-Runge–Kutta, the ASIRK-2A-D is unconditionally stable with respect to the diffusion but the reaction is treated with the explicit Runge–Kutta. Hence these two methods behave almost identically, as seen in Fig. 4 the markers for these two methods are overlapping each other.

But for the new IIF method, the error remains second order accurate for  $\Delta t$  up to 0.5 since the method is unconditionally linearly stable. There exists a large range of  $\Delta t$  at which IIF method converges with reasonable errors, however the other four methods do not converge.

Finally, we test the weighted IIF-ETD method. In order for  $w_2$  to be positive in Eq. (26) and (27), the weight  $w_1$  must be smaller than the bound  $W(q\Delta t)$  in (28). For a system like (2), the bound then becomes a function of the eigenvalue of  $\mathcal{C}$ . In Table 3, we list the bounds associated with the largest and the smallest eigenvalues at various  $\Delta t$  for a fixed  $\mathcal{C}$  resulted from a spatial discretization of the system (34).

Since the bound ranges from 0.007 to 1,  $w_1$  needs to be very small to satisfy all bounds. On the other hand, the stability region for wIIF-ETD becomes very small as  $w_1$  decreases (see Fig. 3). Therefore, it is impractical to require both weights  $w_1$  and  $w_2$  to be positive. Instead, we use three relatively large  $w_1$  values – 0.6, 0.8, 0.95 – to ensure a larger stability region.

As seen in Fig. 4, the case  $w_1 = 0.6$  behaves better than the standard ETD, which is the case corresponding to  $w_1 = 0$ . Similarly, the case  $w_1 = 0.8$  blows up at a larger  $\Delta t$  than the case  $w_1 = 0.6$  due to a larger stability. When  $w_1$  increases to 0.95, the weight for IIF is dominant and the wIIF-ETD becomes unconditionally stable. The maximum error of the solution maintains second order accuracy for very large  $\Delta t$  similar to the IIF scheme. Clearly, for a large  $w_1$ , wIIF-ETD has good stability regions similar to IIF, but it requires evaluation of an inverse of  $\mathcal{C}$  similar to the ETD scheme. Without special treatment described in [4], this calculation leads to loss in accuracy of the ETD scheme. As demonstrated in Fig. 4, when the time step is small enough, the error loses second order accuracy for the schemes containing terms due to the ETD approximation (ETD2, ETD-RK2, wIIF-ETD). It is not the case for the the methods without such terms (RK2, ASIRK-2A, IIF2), and those methods remain second order accurate as long as the solution converges. This problem of ETD can be fixed using contour integral techniques [4] and other methods [5,6], but it demands significant extra calculations.

Among the five methods discussed above, only the IIF and ASIRK methods have implicit treatment on parts of the equations, hence they both require solving linear or nonlinear systems. In the IIF, a nonlinear system with  $m$  unknowns needs to be solved at  $N$  spatial points, whereas in the ASIRK-2A-R, a two stage method, two nonlinear systems each with  $m$  unknowns need to be solved at  $N$  spatial points. In the ASIRK-2A-D, two linear systems each with  $m \cdot N$  unknowns, arising from the implicit treatment of the diffusion, need to be solved. The computational cost *per time step* for the ASIRK-2A-R or the IIF method depends on the choice of the nonlinear solver for the reaction whereas for the ASIRK-2A-D it depends on the choice of spatial discretization on the diffusion in addition to the choice of the linear solver. For the one-dimensional spatial problem in this paper, a second order central difference discretization on the diffusion in the ASIRK-2A-D leads to a tri-diagonal linear system, and it needs only  $O(N)$  operations when Thomas algorithm is used to solve this system.

Table 3  
The bound in Eq. (28) for the smallest and largest eigenvalues associated with the diffusion matrix at various  $\Delta t$

$\Delta t$	$W(q\Delta t)$	
	$q = 538$	$q = 10^{-3}$
$5.0 \times 10^{-1}$	0.007	0.99
$1.0 \times 10^{-1}$	0.04	0.99
$4.0 \times 10^{-2}$	0.09	0.99
$2.0 \times 10^{-2}$	0.18	0.99
$1.0 \times 10^{-2}$	0.36	0.99
$5.0 \times 10^{-3}$	0.64	1.00
$2.5 \times 10^{-3}$	0.87	1.00
$1.25 \times 10^{-3}$	0.96	1.00

Table 4  
CPU time (seconds) per time step for all the methods in Fig. 4 using different  $N$

	$N = 577$	$N = 289$	$N = 145$
IIF2	$1.47 \times 10^{-2}$	$2.77 \times 10^{-3}$	$6.9 \times 10^{-4}$
ETD-RK2	$2.22 \times 10^{-2}$	$5.32 \times 10^{-3}$	$1.26 \times 10^{-3}$
RK2	$5.9 \times 10^{-4}$	$2.8 \times 10^{-4}$	$1.5 \times 10^{-4}$
ASIRK-2A-R	$6.7 \times 10^{-4}$	$3.2 \times 10^{-4}$	$1.6 \times 10^{-4}$
ASIRK-2A-D	$1.1 \times 10^{-3}$	$4.8 \times 10^{-4}$	$2.4 \times 10^{-4}$
ETD2	$3.81 \times 10^{-2}$	$9.92 \times 10^{-3}$	$2.25 \times 10^{-3}$
$w_1 = 0.6$	$3.87 \times 10^{-2}$	$9.96 \times 10^{-3}$	$2.26 \times 10^{-3}$
$w_1 = 0.8$	$3.81 \times 10^{-2}$	$9.94 \times 10^{-3}$	$2.27 \times 10^{-3}$
$w_1 = 0.95$	$3.85 \times 10^{-2}$	$9.95 \times 10^{-3}$	$2.26 \times 10^{-3}$

Now we examine the CPU time *per time step* for all the five methods in Fig. 4 when they are applied to the test problem (see Table 4). Since the reaction terms are linear in the test problem, the computational cost for each method mainly comes from the treatment of the explicit terms and evaluations of the reaction terms. For IF, IIF and ETD methods, the direct implementation of the *explicit* terms, independent of the choice of the spatial discretization of the diffusion, involves matrix–vector multiplications of  $O(N^2)$  operations. With this calculation dominating the cost, all IF or ETD based methods at a fixed time step tends to be more expensive at a large  $N$  than the Runge–Kutta method and both ASIRK methods. This is demonstrated in Table 4 as  $N$  is halved. One interesting observation is that IIF method actually is about twice as fast as the two ETD methods, and it is more than three times faster than the wIIF-ETD. This property is not due to the particular choice of our test problem since IIF always requires fewer than half of the vector–matrix multiplications than the ETD methods or the wIIF-ETD as we see in Eq. (26). A more detailed comparison for the computational cost among ETD or IF based methods will be discussed in the next section for equations with nonlinear reaction terms.

In comparison with wIIF-ETD, IIF is more efficient, and it shows better overall performance even though wIIF-ETD may have slightly smaller error for large  $w_1$  (such as the case of  $w_1 = 0.95$ ). The simple structure of the IIF and its property of unconditional stability with respect to the reactions make this method robust and convenient for implementation.

## 6. Numerical simulations of a morphogen system

We now apply the second order implicit integration factor method (IIF2) to a system of reaction–diffusion equations arising from a biological application. One of the central problems in developmental biology is how uniform fields of cells are transformed into tissues with highly specialized cell types at distinct anatomical positions. In this process, diffusible morphogens produced by certain cells pattern the surrounding tissue through interactions with receptor proteins on the cell membrane. Recently, mathematical modeling, analysis and computations have facilitated the understanding and identification of the underlining biological mechanisms in morphogen systems [10,11,20,13,12]. In this paper, we present a simple system of reaction–diffusion equations to model spatial regulation of Wingless (Wg) morphogen distribution by Dally-like protein (*Dlp*) in an imaginal disc of *Drosophila*.

Motivated by a recent experimental study [21] in which *Dlp* was found to cooperate with *Notum* to limit Wg formation, we include an enzymatic modification of *Dlp* due to *Notum* [22] into a ligand–receptor model [10] similar to the system in [12]. To understand the role of the Dally-like protein *Dlp* on formation of the morphogen gradient, we first examine a simple system to study how a diffusible non-signaling protein, such as the enzymatically modified *Dlp*, affects the morphogen gradient.

Let  $[L]$ ,  $[LR]$ ,  $[N^*]$  and  $[LN^*]$  denote the concentration of Wg, Wg–Dfz2 (the ligand–receptor complex), the enzymatic modification of *Dlp*, and the complex produced by the interaction of Wg and the enzymatic modification of *Dlp*, respectively. The reactions among the proteins are illustrated in Fig. 5.  $\bar{V}_L$  and  $\bar{V}_N$  represent

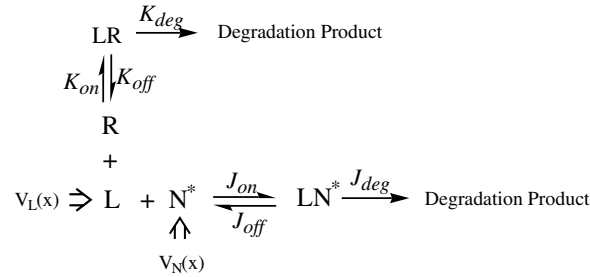


Fig. 5. A reaction diagram for the Wg signal system.

the production rate of  $L$  and  $N^*$  respectively;  $\{K_{on}, J_{on}\}$ ,  $\{K_{off}, J_{off}\}$ ,  $\{K_{deg}, J_{deg}\}$  denote binding rates, off rates, and degradation rates.

$[L]$ ,  $[N^*]$  and  $[LN^*]$  are assumed to have the same diffusion coefficient:  $D$ ; and the total amount receptor,  $Dfz2$ , is assumed to be fixed (see [12]), with a concentration  $R_0$ , such that the free receptor at any given time is  $R_0 - [LR]$ . The mid-point of the Wg production region, the dorsal–ventral boundary, is denoted as  $-\bar{d}$  [10,23] while the edge of the imaginal wing disc in the dorsal–ventral direction is denoted as  $X_{max}$ . The governing equations for the four quantities in  $(-\bar{d}, X_{max})$  then have the following form:

$$\frac{\partial [L]}{\partial T} = D \frac{\partial^2 [L]}{\partial X^2} - K_{on}[L] \cdot (R_0 - [LR]) + K_{off}[LR] - J_{on}[L] \cdot [N^*] + J_{off}[LN^*] + \bar{V}_L(X), \tag{36}$$

$$\frac{\partial [LR]}{\partial T} = K_{on}[L] \cdot (R_0 - [LR]) - (K_{off} + K_{deg})[LR], \tag{37}$$

$$\frac{\partial [LN^*]}{\partial T} = D \frac{\partial^2 [LN^*]}{\partial X^2} + J_{on}[L] \cdot [N^*] - (J_{off} + J_{deg})[LN^*], \tag{38}$$

$$\frac{\partial [N^*]}{\partial T} = D \frac{\partial^2 [N^*]}{\partial X^2} - J_{on}[L] \cdot [N^*] + J_{off}[LN^*] + \bar{V}_N(X). \tag{39}$$

By symmetry of the Wg production region, we have

$$\frac{\partial [L]}{\partial X}(T, -\bar{d}) = 0, \quad \frac{\partial [LN^*]}{\partial X}(T, -\bar{d}) = 0, \quad \frac{\partial [N^*]}{\partial X}(T, -\bar{d}) = 0.$$

Far away from the production region, we assume all the diffusible proteins are absorbed:

$$L(T, X_{max}) = 0, \quad [LN^*](T, X_{max}) = 0, \quad [N^*](T, X_{max}) = 0.$$

In the Wg production region  $[-\bar{d}, 0]$ ,

$$\bar{V}_L(X) = v_L,$$

where  $v_L$  is a constant, and  $\bar{V}_L(X) = 0$  for  $X \in (0, X_{max}]$ . Because  $Dlp$  is produced everywhere,  $\bar{V}_N(X) = v_N$  for  $X \in (-\bar{d}, X_{max})$  with  $v_N$  as a constant.

The system (36)–(39) can be non-dimensionalized with a change of variables [11,12]:

$$\begin{aligned}
 x &= \frac{X}{X_{max}}, \quad t = \frac{D \cdot T}{X_{max}^2}, \\
 \{h_L, h_{LN}\} &= \frac{X_{max}^2 R_0}{D} \cdot \{K_{on}, J_{on}\}, \\
 \{f_L, f_{LN}, g_L, g_{LN}\} &= \frac{X_{max}^2}{D} \cdot \{K_{off}, J_{off}, K_{deg}, J_{deg}\}, \\
 \{V_L(x), V_N(x)\} &= \frac{X_{max}^2}{R_0 D} \cdot \{\bar{V}_L(X), \bar{V}_N(X)\}, \\
 \{A, B, C, D\} &= \frac{1}{R_0} \cdot \{[L], [LR], [LN^*], [N^*]\}.
 \end{aligned}$$

In terms of the normalized quantities, Eqs. (36)–(39) become

$$\frac{\partial A}{\partial t} = \frac{\partial^2 A}{\partial x^2} - h_L A(1 - B) + f_L B - h_{LN} AD + f_{LN} C + V_L(x), \quad (40)$$

$$\frac{\partial B}{\partial t} = h_L A(1 - B) - (f_L + g_L) B, \quad (41)$$

$$\frac{\partial C}{\partial t} = \frac{\partial^2 C}{\partial x^2} + h_{LN} AD - (f_{LN} + g_{LN}) C, \quad (42)$$

$$\frac{\partial D}{\partial t} = \frac{\partial^2 D}{\partial x^2} - h_{LN} AD + f_{LN} C + V_N(x), \quad (43)$$

with the corresponding non-dimensionalized boundary conditions.

We use the second order central difference to approximate the diffusion with evenly spaced  $N + 1$  grid points, then apply the IIF2 to (36)–(39) using the same implementation in Section 6. Fig. 6 depicts the solutions of the morphogen system at every 20 min with an initial condition  $[L] = [LR] = [LN^*] = [N^*] = 0$ . The system, as expected, reaches a steady state with a biologically observed gradient  $[LR]$  [21,22].

In Table 5, we show the accuracy of our implementation by estimating the order of the temporal discretization with a fixed spatial resolution,  $N = 128$ . Since there are no analytical solutions for this system, the order in column 3 of Table 5 is estimated through the maximal difference, defined as “error”, between the solutions at  $T = 30$  min (see column 2 of Table 5) using two different  $\Delta t$  (see column 1 of Table 5). Clearly, the implementation of the IIF2 is second order accurate as seen in column 3 of Table 5.

Next, we study the performance of our IIF implementation, and compare it with two existing second order methods: the standard ETD method (ETD2) and the ETD-Runge–Kutta method (ETD-RK2). The performance of each method is measured by the CPU time each method takes to run up to a stage such that the relative difference between the solution and a pre-calculated steady state is within  $10^{-3}$ . In Table 6, we show the performance of the cases in Fig. 6 for three methods using two different spatial resolutions and four different temporal resolutions.

In this case, the largest and the smallest eigenvalues of the  $4 \times 4$  Jacobian matrix corresponding to the reaction in (40)–(43) at its steady state are  $-0.15$  and  $-6500$ , respectively. The largest and the smallest eigenvalues

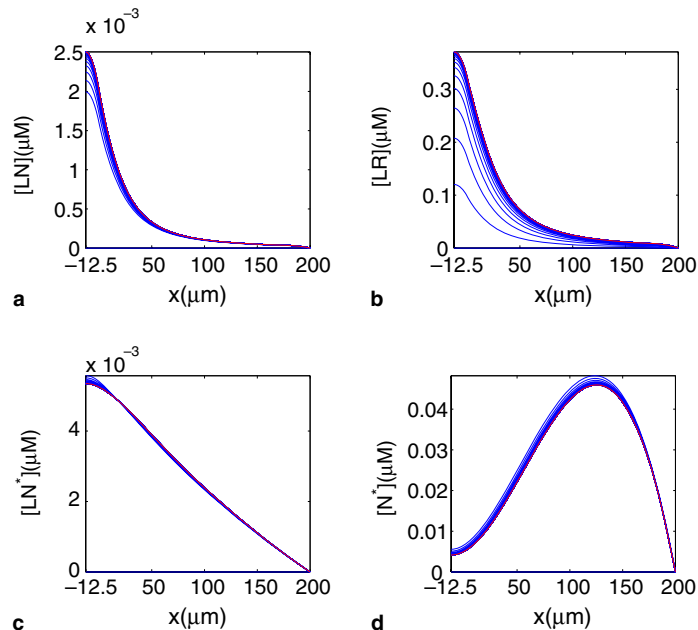


Fig. 6. Dynamics of the morphogen system at every 20 min. In this calculation,  $N = 128$  and  $\Delta t = 10^{-4}$ , and the biological parameters are:  $X_{\max} = 0.02$  cm;  $\bar{d} = 0.125$  cm;  $D = 8.5 \times 10^{-7}$  cm<sup>2</sup>/s;  $K_{\text{on}} = 0.12$  s<sup>-1</sup> μM<sup>-1</sup>;  $K_{\text{off}} = 1.0 \times 10^{-5}$  s<sup>-1</sup>;  $K_{\text{deg}} = 5 \times 10^{-4}$  s<sup>-1</sup>;  $J_{\text{on}} = 285$  s<sup>-1</sup> μM<sup>-1</sup>;  $J_{\text{off}} = 4 \times 10^{-6}$  s<sup>-1</sup>;  $J_{\text{deg}} = 0.54$  s<sup>-1</sup>;  $\bar{V}_L = 8 \times 10^{-4}$  s<sup>-1</sup> μM;  $\bar{V}_N = 2 \times 10^{-3}$  s<sup>-1</sup> μM.

Table 5  
The error and order of accuracy for the second order IIF

$\Delta t$	Error	Order
$1.0 \times 10^{-2}$	$4.86 \times 10^{-6}$	1.78
$5.0 \times 10^{-3}$	$1.41 \times 10^{-6}$	1.97
$1.0 \times 10^{-3}$	$5.96 \times 10^{-8}$	1.99
$5.0 \times 10^{-4}$	$1.49 \times 10^{-8}$	–

for the diffusion matrix  $\mathcal{C}$  at the steady state are  $-2.2$  and  $-1.4 \times 10^4$ , respectively, for  $N = 64$ ; and  $-880$  and  $-5.7 \times 10^6$ , respectively, for  $N = 128$ . Because all three methods are unconditionally stable with respect to the diffusion, the stability constraint on the time step comes solely from the stiff nonlinear reactions.

Since the ETD2 method has a small stability region, it blows up for the two large  $\Delta t$  values, similar to the test problem in Section 5. ETD-RK2 has a better stability region but it still blows up for the largest  $\Delta t$  in Table 6. Only IIF2 converges for all  $\Delta t$  and  $N$  since it is unconditionally stable with respect to reaction. Among all the cases for which all methods converge, IIF2 takes about one half of the CPU time of the other two methods. This indicates that the computational time associated with solving the  $m \times m$  nonlinear system in IIF is relatively small compared to the other cost. Indeed, with a fixed point iterative procedure for solving this system, only about five iterations are needed to find a solution within a  $10^{-10}$  accuracy. Most importantly, the order of calculations associated with such an iteration procedure is  $O(N)$ , whereas the rest of the calculation is  $O(N^2)$  for all three methods. This is confirmed by the fact that the CPU time for all three methods increases by a factor of four as  $N$  doubled. The order of  $N^2$  computational time comes from matrix–vector multiplications with dimension  $m \cdot N$ ; In particular, both ETD2 and ETD-RK2 require more calculations of this kind than IIF2.

Finally, we study how loss of  $Dlp$  locally affects the Wg signal. As shown in the experiment [22], mutation of  $Dlp$  can modestly reduce the activation of Wg signaling where Wg levels are low. To mimic the genetic mutation of  $Dlp$  in [22], we set  $v_N(x)$  to zero in a part of the domain ( $75 \mu\text{m}, 125 \mu\text{m}$ ), and use the case in Fig. 6 as the wild type, that is, all other biological parameters are chosen to be the same as those in Fig. 6. Here, the Wg signal is modeled as the product of the concentration of  $[LR]$  and a co-receptor term due to presence of  $Dlp$  [24]:

$$[\text{Signal}] = [LR] \left( 1 + \frac{c_1([N^*] + [LN^*])^p}{c_2 + ([N^*] + [LN^*])^p} \right). \tag{44}$$

In Fig. 7(a), the Wg signal, modeled as described in (44), is plotted at 3.2 h. The solution at this time, calculated using  $N = 128$  and  $\Delta t = 10^{-2}$ , with  $c_1 = 1000$ ,  $c_2 = 0.00001$ ,  $p = 4$ , is within the steady-state error of  $10^{-3}$ . The two peaks of the signal near the boundary of the clone region, ( $75 \mu\text{m}, 125 \mu\text{m}$ ), have been observed in the experiments (see Fig. 6 in [22]). In addition, as demonstrated in Fig. 7 (b), the two spatial signal peaks increase quickly in time and become much stronger than their neighbors, while the signal at the middle of the clone, which is weaker than the non-clone regions, grows very slowly. This suggests that enzymatic modification of  $Dlp$  through *Notum* can affect the Wg signals and ultimately, patterning activity. In this paper, the enzymatic modification is only modeled through a diffusible non-receptor protein,  $N^*$ . A more comprehensive model and a systematic study on the roles of  $Dlp$  and *Notum* are currently under study, and the results will be presented in a separate paper.

Table 6  
CPU time (minutes) for three different methods

$\Delta t$	ETD2		ETD-RK2		IIF2	
	$N = 64$	$N = 128$	$N = 64$	$N = 128$	$N = 64$	$N = 128$
$5.0 \times 10^{-2}$	NC	NC	NC	NC	1.1	4.3
$2.0 \times 10^{-2}$	NC	NC	5.1	21.9	2.4	8.7
$1.0 \times 10^{-2}$	10	41	10.3	43.8	4.8	17.8
$5.0 \times 10^{-3}$	20	81.5	20.7	87.5	9.6	35.6

“NC” denotes that the method does not converge.

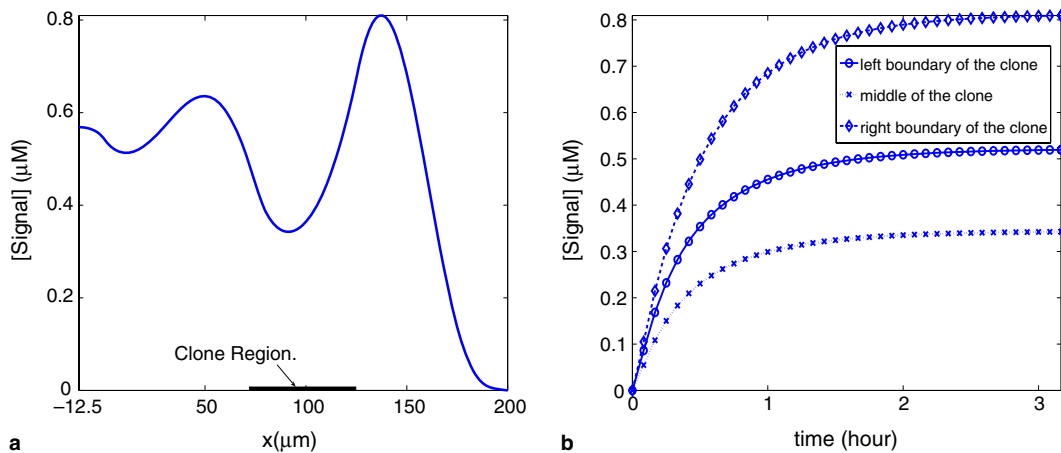


Fig. 7. *Dlp* clones reduce Wg signaling where Wg levels are low: (a) Wg signal near the steady state; (b) time evolution of Wg signal near the boundary of the clone and at the middle of the clone.

## 7. Discussions and conclusions

When temporal schemes are applied to evolution equations of the form (2), the size of the time step is restricted by (a) the linear part  $\mathcal{L}$ , which usually arises from the approximation of diffusions or the term of high-order derivatives, and (b) stiff nonlinear reactions in  $\mathcal{F}$ . The restriction (a) can be removed if the linear part is treated exactly using methods such as integration factor or exponential time differencing. Those methods are efficient for diffusion dominated problem since the treatment of the nonlinear reactions in those methods is still explicit. Although, there have been attempts to treat the nonlinear reactions implicitly using implicit–explicit Runge–Kutta schemes [18,19,25], the diffusion term in those methods is still treated explicitly, hence restriction (a) remains unchanged.

In this paper, we have presented a class of methods which removes both restrictions in the setting of linear stability theory. Most importantly, in the new methods, the nonlinear system due to the implicit treatment of the nonlinear reaction has the same size as the number of original differential equations. This feature together with its stability property makes this type of methods particularly efficient. The new methods would be more advantageous for systems in higher spatial dimensions or systems involving high order derivatives than the studied one-dimensional system with diffusions in the paper. For those systems, a fully implicit method would require solving very large nonlinear systems depending on two- or three-dimensional spatial discretizations. On the other hand, severe time step constraints due to any stiff nonlinear reactions still limit the efficiency of any explicit ETD (or IF) methods.

## Acknowledgments

This research work was supported by the NSF DMS-0511169 Grant, and NIH/NSF initiatives on Mathematical Biology through Grants R01GM57309 and R01GM67247 from the National Institute of General Medical Science. We thank Arthur Lander, Chi-Wang Shu and Fred Wan for stimulating and helpful discussions.

## References

- [1] T.Y. Hou, J.S. Lowengrub, M.J. Shelley, Removing the stiffness from interfacial flows with surface tension, *J. Comput. Phys.* 114 (1994) 312.
- [2] G. Beylkin, J.M. Keiser, On the adaptive numerical solution of nonlinear partial differential equations in wavelet bases, *J. Comput. Phys.* 132 (1997) 233–259.
- [3] G. Beylkin, J.M. Keiser, L. Vozovoi, A new class of time discretization schemes for the solution of nonlinear PDEs, *J. Comput. Phys.* 147 (1998) 362–387.

- [4] A.-K. Kassam, L.N. Trefethen, Fourth-order time stepping for stiff PDEs, *SIAM J. Sci. Comput.* 26 (4) (2005) 1214–1233.
- [5] Q. Du, W. Zhu, Stability analysis and applications of the Exponential Time Differencing Schemes, *J. Comput. Math.* 22 (2004) 200.
- [6] Q. Du, W. Zhu, Modified exponential time differencing schemes: analysis and applications, *BIT, Numer. Math.* 45 (2) (2005) 307–328.
- [7] Q. Du, W. Zhu, Exponential time differencing schemes for parabolic equations: stability analysis and applications of the exponential time differencing schemes, *J. Comput. Math.* 22 (2004) 200–209.
- [8] P.H. Leo, J.S. Lowengrub, Qing Nie, Microstructural evolution in orthotropic elastic media, *J. Comput. Phys.* 157 (2000) 44–88.
- [9] S.M. Cox, P.C. Matthews, Exponential time differencing for stiff systems, *J. Comput. Phys.* 176 (2002) 430–455.
- [10] A. Lander, Q. Nie, F. Wan, Do Morphogen gradients arise by diffusion? *Dev. Cell* 2 (2002) 785–796.
- [11] J. Kao, Q. Nie, A. Teng, F.Y.M. Wan, A.D. Lander, J.L. Marsh, Can morphogen activity be enhanced by its inhibitors? in: *Proceedings of 2nd MIT Conference on Computational Mechanics, 2003*, pp. 1729–1733.
- [12] Y. Lou, Q. Nie, F. Wan, Effects of sog on Dpp-receptor binding, *SIAM J. Appl. Math.* 66 (5) (2005) 1748–1771.
- [13] C. Mizutani, Q. Nie, F. Wan, Y. Zhang, P. Vilmos, E. Bier, L. Marsh, A. Lander, Formation of the bmp activity gradient in the drosophila embryo, *Dev. Cell* 8 (6) (2005) 915–924.
- [14] J. Stoer, R. Bulirsch, *Introduction to Numerical Analysis*, Springer, New York, 1992.
- [15] C. Moler, C.V. Loan, Nineteen dubious ways to compute the exponential of a matrix, twenty-five years later, *SIAM Rev.* 45 (2003) 3–49.
- [16] H.J. Jou, P.H. Leo, J.S. Lowengrub, Microstructural evolution in inhomogeneous elastic media, *J. Comput. Phys.* 131 (1997) 109.
- [17] G.E. Karniadakis, M. Israeli, S.A. Orszag, High order splitting methods for the incompressible Navier–Stokes equations, *J. Comput. Phys.* 97 (1991) 414.
- [18] Xiaolin Zhong, Additive semi-implicit Runge–Kutta methods for computing high-speed nonequilibrium reactive flows, *J. Comput. Phys.* 128 (1996) 19–31.
- [19] C.A. Kennedy, M.H. Carpenter, Additive Runge–Kutta schemes for convection–diffusion–reaction equations, *Appl. Numer. Math.* 44 (2003) 139–181.
- [20] A. Lander, Q. Nie, F. Wan, Membrane associated non-receptors and morphogen gradients, *Bull. Math. Biol.* (2005), accepted for publication.
- [21] C.A. Kirkpatrick, B.D. Dimitroff, J.M. Rawson, S.B. Selleck, Spatial regulation of wingless morphogen distribution and signaling by Dally-like protein, *Dev. Cell* 7 (2004) 513–523.
- [22] A.J. Giraldez, R.R. Copley, S.M. Cohen, HSPG modification by the secreted enzyme Notum shapes the Wingless morphogen gradient, *Dev. Cell* 2 (2002) 667–676.
- [23] A. Lander, Q. Nie, F. Wan, Spatially distributed morphogen production and morphogen gradient formation, *Math. Biosci. Eng.* 2 (2) (2005) 239–262.
- [24] S.B. Selleck, Proteoglycans and pattern formation – sugar biochemistry meets developmental genetics, *Trends Genet.* 16 (5) (2000) 206–212.
- [25] J.G. Verwer, B.P. Sommeijer, An implicit–explicit Runge–Kutta–Chebyshev scheme for diffusion–reaction equations, *SIAM J. Sci. Comput.* 25 (2004) 1824–1835.